Research Article

Mehmet Tahir Gulluoglu*

New Complex Solutions to the Nonlinear Electrical Transmission Line Model

https://doi.org/10.1515/phys-2019-0074
Received Sep 11, 2019; accepted Oct 10, 2019

Abstract: In this paper, with the help of an analytical approach, new complex singular and travelling dark solutionsto the nonlinear electrical transmission line are successfully constructed. 2D and 3Dfigures along with contour figures are plotted. Finally, at the end of manuscript, general conclusions about these novel findings, which differ from existing results, are given.

Keywords: Nonlinear electrical transmission line equation, Improved Bernoulli sub-equation function method, Complex solutions, Contour surfaces

PACS: 02.30.Jr, 02.30.Hq

1 Introduction

Energy is one of the most important requirementsof people from all over the world. "*The demand for energy and natural resources is increasing rapidly in conjunction with rising population, industrialization, and urbanization as well as the growth in production and commercial opportunities resulting from globalization* [1]." Furthermore, networks, which are related to energy, are another requirement for people. Therefore, they are an outstanding connection tool among people in the modern day. These two concepts,energy and networks, are used in many fields of science and real world problems arising in all aspect of daily life.Research conducted on these fields has attracted the attention of scientists from all over the world, and continues to be studied in the literature.

H. Reda *et al.* have investigated the wave propagation in pre-deformed periodic network materials based on large strains homogenization [2]. Wave emitting and propagation on neural networks have been investigated by J. Ma *et al.* in 2015 [3]. Z. Rostami *et al.* have studied a deep searchfor propagating waves in a neural network using magnetic radiation [4]. Denys Dutykh and Jean-Guy Caputo have observedwave propagation on the wave dynamics on networks [5]. Atte Aalto and Jarmo Malinen have introduced that wave propagation on networks solvable (forward in time) and energy passive or conservative with the help of a theoretical approach [6]. Therefore, many novel models have been presented to the literature by many scientists [14–32].

One such novel model, voltage wave propagation of electrical transmission lines, has been presented by E. Tala-Tebue as

$$\begin{aligned} v_{tt} - \alpha\left(v^2\right)_{tt} + \beta\left(v^3\right)_{tt} - \varpi_0^2\delta_1^2 v_{xx} - \varpi_0^2\frac{\delta_1^4}{12}v_{xxxx} \\ - \omega_0^2\delta_2^2 v_{yy} - \omega_0^2\frac{\delta_2^4}{12}v_{yyyy} = 0, \end{aligned} \tag{1}$$

where α, β, ϖ_0, δ_1, ω_0, δ_2 are real, non-zero constants while $v = v(x, y, t)$ is the voltage in the transmission lines [7, 8]. This nonlinear electrical transmission line model (NETLM) has been used to symbolize the wave propagation on the network system [7, 8].

This manucript is composed of the following three sections. In section 2, we present the Improved Bernoulli Sub-Equation function method (IBSEFM) in a detailed manner. We apply IBSEFM to find new complex travelling wave solution in section 3. In the last section of paper, we introduce a comprehensive conclusion.

2 General properties of IBSEFM

The general properties of IBSEFM are given as follows:

Step 1. The following nonlinear model in two variables and a dependent variable u can be considered:

$$P\left(v_x, v_y, v_t, v_{xyt}, \cdots\right) = 0, \tag{2}$$

and taking the travelling wave transformation

$$v(x, y, t) = V(\xi), \quad \xi = k(x + y - ct), \tag{3}$$

in which k, c are real constants and non-zero. Substituting Eq. (3) in Eq. (2) yields a nonlinear ordi-

***Corresponding Author: Mehmet Tahir Gulluoglu:** Department of Electrical and Electronics Engineering, Faculty of Engineering, Harran University, Sanliurfa, Turkey; Email: mtahir@harran.edu.tr

nary differential equation (NLODE) as follows;

$$N\left(V, V', V'', \cdots\right) = 0, \tag{4}$$

where $V = V(\xi)$, $V' = \frac{dV}{d\xi}$, $V'' = \frac{d^2V}{d\xi^2}, \cdots$.

Step 2. Taking the trial solution for Eq. (4) as follows [9–13]:

$$V = \frac{\sum_{i=0}^{n} a_i F^i}{\sum_{j=0}^{m} b_j F^j} = \frac{a_0 + a_1 F + a_2 F^2 + \cdots + a_n F^n}{b_0 + b_1 F + b_2 F^2 + \cdots + b_m F^m}, \tag{5}$$

and

$$F' = pF + dF^M, \tag{6}$$

where $F = F(\xi)$ is a Bernoulli differential polynomial and $p \neq 0$, $d \neq 0$, $M \in -\{0, 1, 2\}$. Putting Eqs. (5, 6) into Eq. (4) produces an equation of polynomial $\Omega(F)$of F as follows:

$$\Omega(F) = \rho_s F^s + \cdots + \rho_1 F + \rho_0 = 0. \tag{7}$$

We can obtain a relationship between n, m and M under the rules of the balance principle.

Step 3. Setting the coefficients of $\Omega(F)$ all equal to zero gives an algebraic system of equations;

$$\rho_i = 0, \; i = 0, \cdots, s. \tag{8}$$

Solving this system, we obtain the values of $a_0, a_1, \cdots, a_n$ and $b_0, b_1, \cdots, b_m$

Step 4. When we solve Eq. (6), we obtain the following two situations according to the values of p and d;

$$F(\xi) = \left[\frac{-d}{p} + \frac{E}{e^{p(M-1)\xi}}\right]^{\frac{1}{1-M}}, \; p \neq d, \tag{9}$$

$$F(\xi) = \left[\frac{(E-1) + (E+1)\tanh\left(\frac{p(1-M)\xi}{2}\right)}{1 - \tanh\left(\frac{p(1-M)\xi}{2}\right)}\right]^{\frac{1}{1-M}}, \tag{10}$$

$p = d$, $E \in$.

Substituting Eq. (5) into Eq. (4), we can find the polynomial of F. Considering all the coefficients of the same power of F to be zero gives an algebraic system of equations. By solving this system with the help of various computational programs, we can find some new values of parameters. This process gives many solutions to the model considered. For a better understanding of the solutions obtained in this manner, we plot 2D, 3D and contour graphs of results with the suitable values of parameters.

3 Application of the IBSEFM

In this section, IBSEFM has been successfully considered to the NETLM to find additional novel complex solutions.

Example: Let's consider the travelling wave transformation as following;

$$v = v(x, y, t) = V(\xi), \quad \xi = k(x + y - ct), \tag{11}$$

where k, c are real constants and non-zero. Substituting Eq. (11) into Eq. (1) produces the following *NLODE*;

$$\begin{aligned}&\left[c^2 - \omega_0^2\delta_2^2 - \varpi_0^2\delta_1^2\right] k^2 V'' - 2\alpha k^2 c^2 \left[VV'\right]' \\ &+ 3\beta k^2 c^2 \left[V^2 V'\right]' - \left[\varpi_0^2\delta_1^4 + \omega_0^2\delta_2^4\right] \frac{k^4}{12} V^{(4)} = 0.\end{aligned} \tag{12}$$

Integrating twice and considering the zero for both constants, Eq. (12) can be rewritten as

$$\begin{aligned}&12\left[c^2 - \varpi_0^2\delta_1^2 - \omega_0^2\delta_2^2\right] V + 12\beta c^2 V^3 - 12\alpha c^2 V^2 \\ &- k^2\left[\varpi_0^2\delta_1^4 + \omega_0^2\delta_2^4\right] V'' = 0\end{aligned} \tag{13}$$

With the balance principle for V'' and V^3, we obtain the relationship among n, m and M as

$$M + m = n + 1. \tag{14}$$

Case 1: Choosing $M = 3$, $n = 3$ and $m = 1$, we can find V and its derivatives from Eq. (5) as follows:

$$V = \frac{a_0 + a_1 F + a_2 F^2 + a_3 F^3}{b_0 + b_1 F} = \frac{Y}{\Psi}, \tag{15}$$

$$V' = \frac{Y'\Psi - Y\Psi'}{\Psi^2}, \tag{16}$$

$$V'' = \frac{Y''\Psi - Y\Psi'}{\Psi^2} - \frac{\left(Y\Psi'\right)'\Psi^2 - 2Y\left(\Psi'\right)^2\Psi}{\Psi^4}, \tag{17}$$

$$\vdots$$

where $F' = pF + dF^3$, $a_3 \neq 0$, $b_1 \neq 0$, $p \neq 0$, $d \neq 0$. When we use Eq. (17) in Eq. (13), we obtain a system of algebraic equations. By solving this system of equations with the help of software programs, we find the coefficients, which give the complex solutions to the NETLM as follows.

Case 1a.

$$\begin{aligned}&a_0 = \frac{pa_2}{d}, \quad a_1 = \frac{pa_2 b_1}{db_0}, \quad a_3 = \frac{a_2 b_1}{b_0}, \\ &c = \sqrt{\frac{2d^2 b_0^2\left(w_0^2\delta_1^2 + \omega_0^2\delta_2^2\right)}{-p^2\beta a_2^2 + 2d^2 b_0^2}}, \quad \alpha = \frac{3p\beta a_2}{2db_0}, \\ &k = \frac{-ia_2\sqrt{3\beta}\sqrt{w_0^2\delta_1^2 + \delta_2^2\omega_0^2}}{\sqrt{\left(p^2\beta a_2^2 - 2d^2 b_0^2\right)\left(w_0^2\delta_1^4 + \delta_2^4\omega_0^2\right)}},\end{aligned} \tag{18}$$

we have

$$v_1(x,y,t) = \frac{E a_2 p^2 e^{i \frac{2a_2\sqrt{3\beta}\sqrt{w_0^2\delta_1^2+\delta_2^2\omega_0^2}}{\sqrt{\left(p^2\beta a_2^2-2d^2b_0^2\right)\left(w_0^2\delta_1^4+\delta_2^4\omega_0^2\right)}}\left(x+y-\sqrt{2}t\sqrt{\frac{d^2b_0^2\left(w_0^2\delta_1^2+\omega_0^2\delta_2^2\right)}{-p^2\beta a_2^2+2d^2b_0^2}}\right)}}{-b_0d^2+pdEb_0 e^{i \frac{2a_2\sqrt{3\beta}\sqrt{w_0^2\delta_1^2+\delta_2^2\omega_0^2}}{\sqrt{\left(p^2\beta a_2^2-2d^2b_0^2\right)\left(w_0^2\delta_1^4+\delta_2^4\omega_0^2\right)}}\left(x+y-\sqrt{2}t\sqrt{\frac{d^2b_0^2\left(w_0^2\delta_1^2+\omega_0^2\delta_2^2\right)}{-p^2\beta a_2^2+2d^2b_0^2}}\right)}}. \tag{19}$$

For a better understanding of the physical meaning of the solution with the help of the complex structure of Eq. (19) in Eq. (1), and with suitable values of parameters, 2D and 3D figures along with contour graphs may be observed in Figures 1, 2, 3, 4.

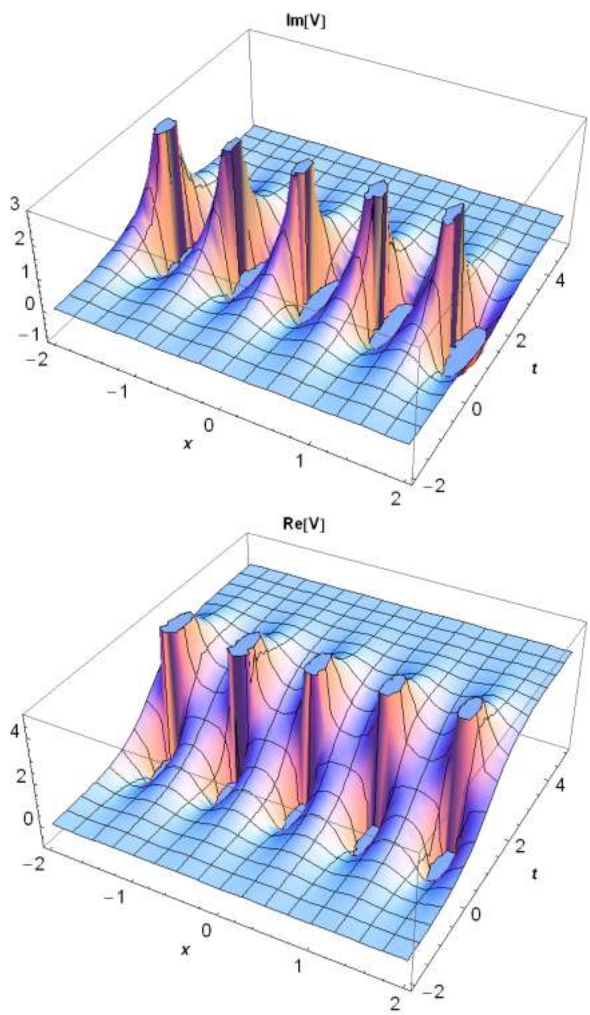

Figure 1: The 3D graphs of Eq. (19) for $a_2 = 0.9$, $d = 0.2$, $b_0 = b_1 = 0.3$, $p = 0.25$, $\delta_1 = \delta_2 = 0.5$, $\beta = 0.9$, $E = 0.1$, $w_0 = 0.7$, $\omega_0 = 0.8$, $y = 0.03$, $-2 < x < 2$, $-2 < t < 5$.

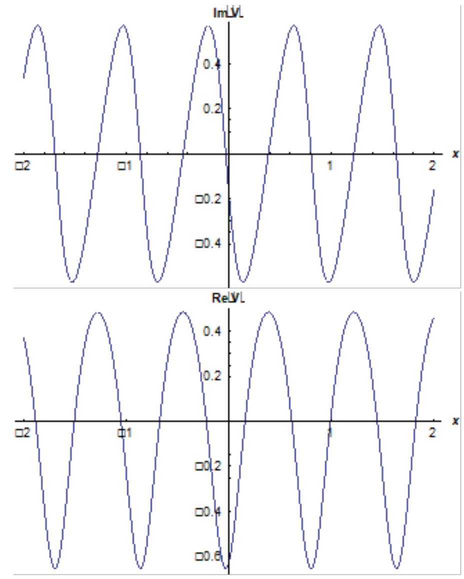

Figure 2: The 2D graphs of Eq. (19) for $a_2 = 0.9$, $d = 0.2$, $b_0 = b_1 = 0.3$, $p = 0.25$, $\delta_1 = \delta_2 = 0.5$, $\beta = 0.9$, $E = 0.1$, $w_0 = 0.7$, $\omega_0 = 0.8$, $y = 0.03$, $t = 0.1$, $-2 < x < 2$

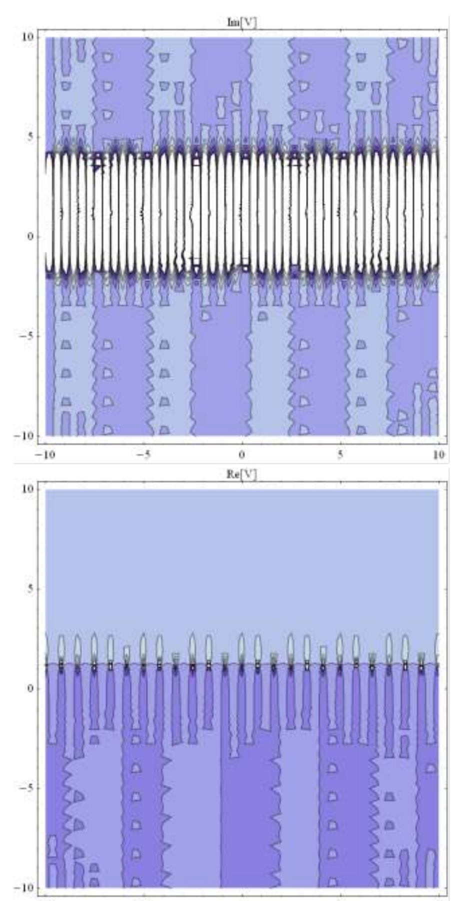

Figure 3: The contour graphs of Eq. (19) for $a_2 = 0.9$, $d = 0.2$, $b_0 = b_1 = 0.3$, $p = 0.25$, $\delta_1 = \delta_2 = 0.5$, $\beta = 0.9$, $E = 0.1$, $w_0 = 0.7$, $\omega_0 = 0.8$, $y = 0.03$, $-10 < x < 10$, $-10 < t < 10$.

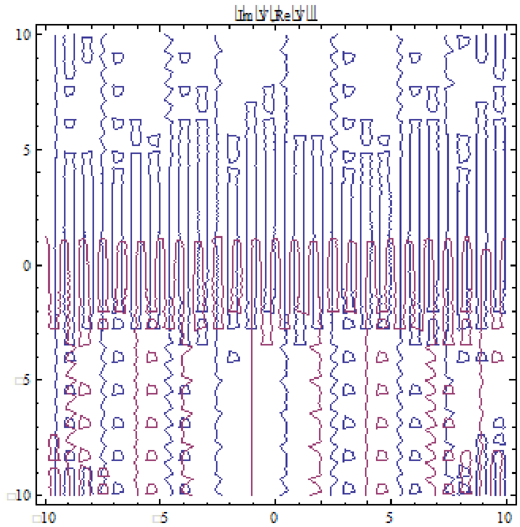

Figure 4: The compilation of contour graphs of both side of Eq. (19) for $a_2 = 0.9, d = 0.2, b_0 = b_1 = 0.3, p = 0.25, \delta_1 = \delta_2 = 0.5, \beta = 0.9, E = 0.1, w_0 = 0.7, \omega_0 = 0.8, y = 0.03, -10 < x < 10, -10 < t < 10.$

Case 1b. When

$$a_0 = a_1 = 0, \quad a_3 = \frac{a_2 b_1}{b_0}, \tag{20}$$
$$c = -\frac{\sqrt{w_0^2\delta_1^2\left(3 + k^2p^2\delta_1^2\right) + \omega_0^2\delta_2^2\left(3 + k^2p^2\delta_2^2\right)}}{\sqrt{3}},$$
$$\alpha = \frac{-3dk^2pb_0\left(w_0^2\delta_1^4 + \delta_2^4\omega_0^2\right)}{a_2w_0^2\delta_1^2\left(3 + k^2p^2\delta_1^2\right) + a_2\omega_0^2\delta_2^2\left(3 + k^2p^2\delta_2^2\right)},$$
$$\beta = \frac{2d^2k^2b_0^2\left(w_0^2\delta_1^4 + \delta_2^4\omega_0^2\right)}{a_2^2w_0^2\delta_1^2\left(3 + k^2p^2\delta_1^2\right) + a_2^2\omega_0^2\delta_2^2\left(3 + k^2p^2\delta_2^2\right)},$$

we find the dark solitary wave structure as following;

$$v_2(x, y, t) = pa_2\left(-db_0 + pb_0E\frac{\sqrt{-1 - \tanh\left(-2kpx - 2kpy - 2kpt\varpi\right)}}{\sqrt{-1 + \tanh\left(-2kpx - 2kpy - 2kpt\varpi\right)}}\right)^{-1}, \tag{21}$$

where $\varpi = \frac{\sqrt{w_0^2\delta_1^2(3+k^2p^2\delta_1^2)+\omega_0^2\delta_2^2(3+k^2p^2\delta_2^2)}}{\sqrt{3}}$. With the suitable values of parameters, 2D and 3D figures along with contour graphs may be observed in Figures 5, 6.

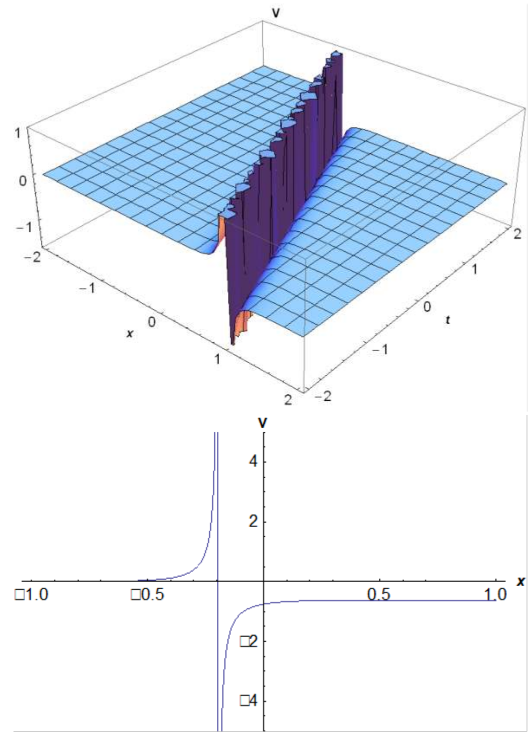

Figure 5: The 2D and 3D graphs of Eq. (21) for $a_2 = 1, d = 2, b_0 = 4, b_1 = 3, p = 5, k = 0.9, \delta_1 = \delta_2 = 0.3, E = 2, w_0 = 0.7, \omega_0 = 0.8, y = 0.03, -2 < x < 2, -2 < t < 2$, and $t = 0.85$ for 2D surfaces.

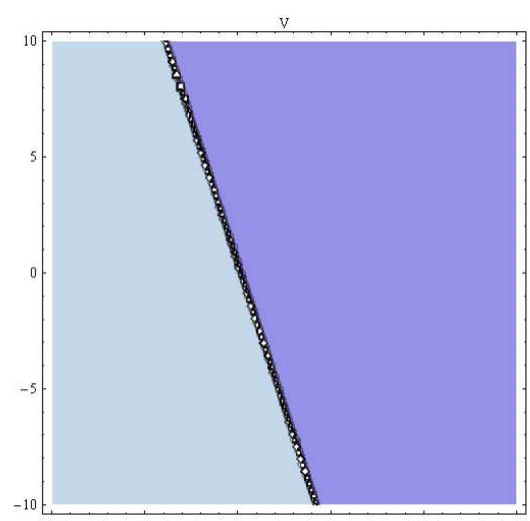

Figure 6: The contour graphs of Eq. (21) for$a_2 = 1, d = 2, b_0 = 4, b_1 = 3, p = 5, k = 0.9, \delta_1 = \delta_2 = 0.3, E = 2, w_0 = 0.7, \omega_0 = 0.8, y = 0.03, -2 < x < 2, -2 < t < 2.$

Case 1c. If we consider

$$a_0=\frac{3b_0\left(c^2-w_0^2\delta_1^2-\omega_0^2\delta_2^2\right)}{c^2\alpha},\tag{22}$$
$$a_1=\frac{3b_1\left(c^2-w_0^2\delta_1^2-\omega_0^2\delta_2^2\right)}{c^2\alpha},\quad a_3=\frac{a_2b_1}{b_0},$$
$$p=\frac{3db_0\left(c^2-w_0^2\delta_1^2-\omega_0^2\delta_2^2\right)}{c^2\alpha a_2},$$
$$k=\frac{-ic^2\alpha a_2}{\sqrt{3d^2b_0^2\left(c^2-w_0^2\delta_1^2-\omega_0^2\delta_2^2\right)\left(w_0^2\delta_1^4+\delta_2^4\omega_0^2\right)}},$$
$$\beta=\frac{2c^2\alpha^2}{9\left(c^2-w_0^2\delta_1^2-\omega_0^2\delta_2^2\right)},$$

we obtain another new complex dark solitary wave structure as

$$v_3(x,y,t)=\frac{3}{\alpha}-\frac{3\left(w_0^2\delta_1^2+\omega_0^2\delta_2^2\right)}{\alpha c^2}\tag{23}$$
$$+\frac{\sqrt{-1+\tanh(2i\varpi(x+y-ct))}}{-\frac{\alpha c^2}{3\zeta}\sqrt{-1+\tanh(2i\varpi(x+y-ct))}+\frac{Eb_0}{a_2}\sqrt{-1-\tanh(2i\varpi(x+y-ct))}},$$

where $\zeta=c^2-w_0^2\delta_1^2-\omega_0^2\delta_2^2$, $\varpi=\frac{\sqrt{3}db_0\sqrt{\zeta}}{\kappa}$, $\kappa=\sqrt{-d^2b_0^2\left(w_0^2\delta_1^4+\delta_2^4\omega_0^2\right)}$. For suitable values of parameters, 2D and 3D figures along with contour graphs the complex structure Eq. (23) with Eq. (1) may be observed in Figures 7, 8, 9, 10.

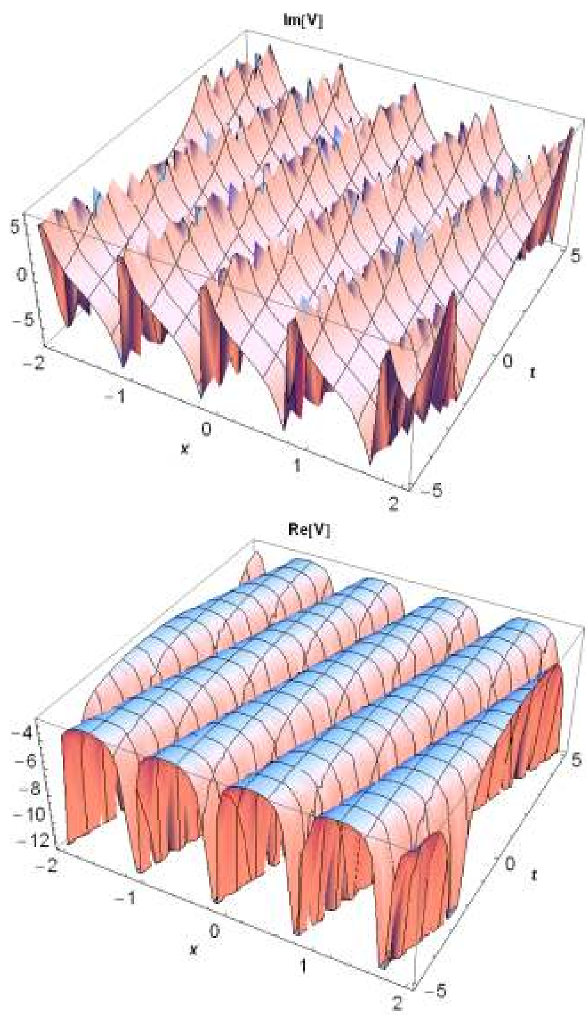

Figure 7: The 3D graphs of Eq. (23) for $a_2=0.1$, $d=-0.2$, $b_0=b_1=0.3$, $c=0.12$, $\delta_1=\delta_2=0.5$, $\alpha=12$, $E=0.1$, $w_0=0.7$, $\omega_0=0.8$, $y=0.03$, $-2<x<2$, $-5<t<5$.

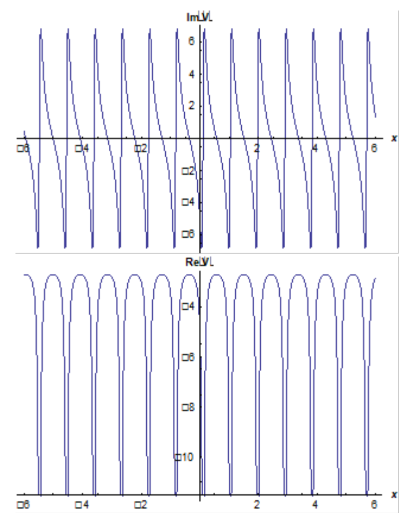

Figure 8: The 2D graphs of Eq. (23) for $a_2=0.1$, $d=-0.2$, $b_0=b_1=0.3$, $c=0.12$, $\delta_1=\delta_2=0.5$, $\alpha=12$, $E=0.1$, $w_0=0.7$, $\omega_0=0.8$, $y=0.03$, $t=5$, $-6<x<6$.

Case 1d. Taking

$$a_0=a_1=0,\quad a_2=\frac{a_3b_0}{b_1},\tag{24}$$
$$p=\frac{3db_1\left(-c^2+w_\theta^2\delta_1^2+\delta_2^2\omega_\theta^2\right)}{c^2\alpha a_3},$$
$$k=\frac{-ic^2\alpha a_3}{\sqrt{-3d^2b_1^2\left(c^2-w_0^2\delta_1^2-\omega_0^2\delta_2^2\right)\left(w_0^2\delta_1^4+\delta_2^4\omega_0^2\right)}},$$
$$\beta=\frac{2c^2\alpha^2}{9\left(c^2-w_0^2\delta_1^2-\omega_0^2\delta_2^2\right)},$$

we find another new complex wave structure as

$$v_4(x,y,t)=\tag{25}$$
$$\frac{a_3\left(3c^2-3w_0^2\delta_1^2-3\omega_0^2\delta_2^2\right)}{Eb_1\left(3c^2-3w_0^2\delta_1^2-3\omega_0^2\delta_2^2\right)e^{\frac{-2idb_1\sqrt{3}\sqrt{c^2-w_0^2\delta_1^2-\omega_0^2\delta_2^2}}{\sqrt{d^2b_1^2\left(-w_0^2\delta_1^4-\delta_2^4\omega_0^2\right)}}(x+y-ct)}+c^2\alpha a_3}.$$

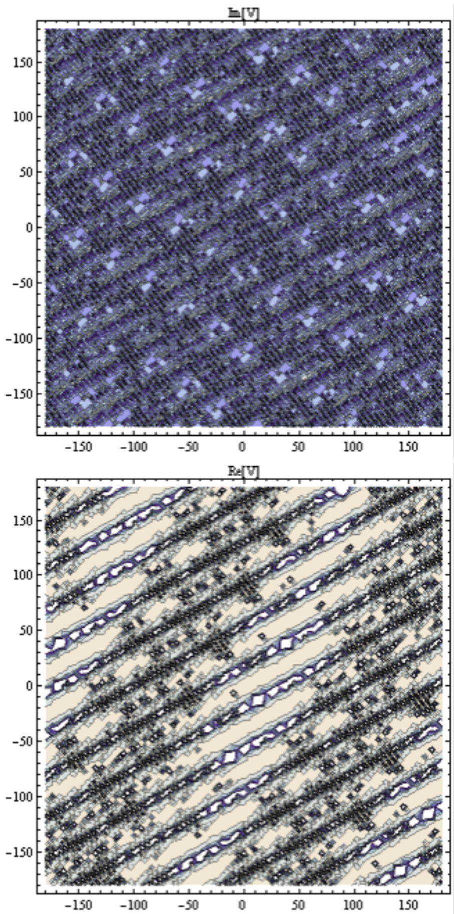

Figure 9: The contour graphs of Eq. (23) for $a_2 = 0.1$, $d = -0.2$, $b_0 = b_1 = 0.3$, $c = 0.12$, $\delta_1 = \delta_2 = 0.5$, $\alpha = 12$, $E = 0.1$, $w_0 = 0.7$, $\omega_0 = 0.8$, $y = 0.03$, $-180 < x < 180$, $-180 < t < 180$.

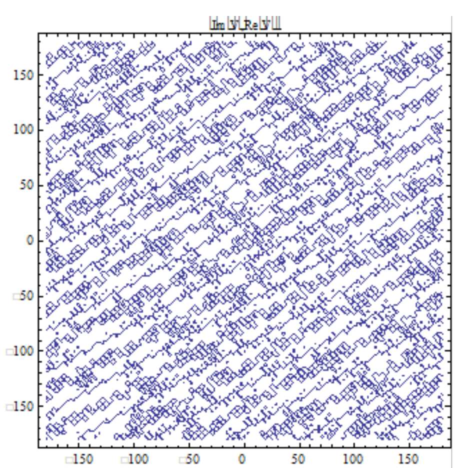

Figure 10: The compilation of contour graphs of both sides of Eq. (23) for $a_2 = 0.1$, $d = -0.2$, $b_0 = b_1 = 0.3$, $c = 0.12$, $\delta_1 = \delta_2 = 0.5$, $\alpha = 12$, $E = 0.1$, $w_0 = 0.7$, $\omega_0 = 0.8$, $y = 0.03$, $-180 < x < 180$, $-180 < t < 180$.

2D and 3D figures along with contour graphs for the complex structure Eq. (25) in Eq. (1) may be seen in Figures 11, 12, 13, 14.

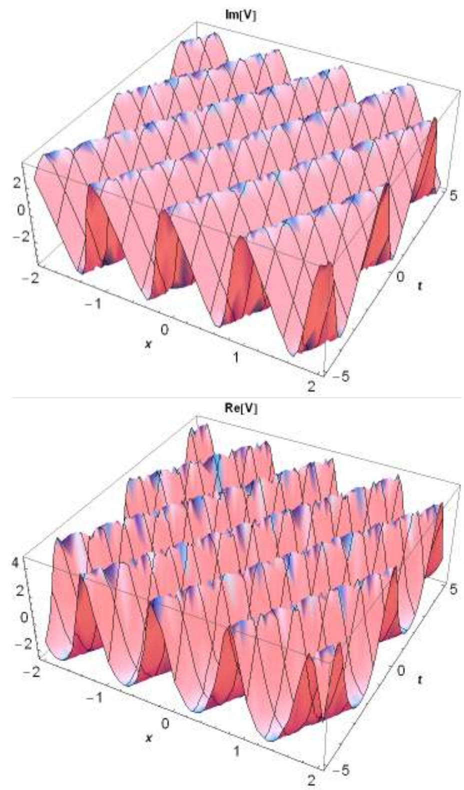

Figure 11: The 3D graphs of Eq. (25) for $a_3 = 0.1$, $d = -0.2$, $b_0 = b_1 = 0.3$, $c = 0.25$, $\delta_1 = \delta_2 = 0.5$, $\alpha = 0.9$, $E = 0.1$, $w_0 = 0.7$, $\omega_0 = 0.8$, $y = 0.03$, $-2 < x < 2$, $-5 < t < 5$.

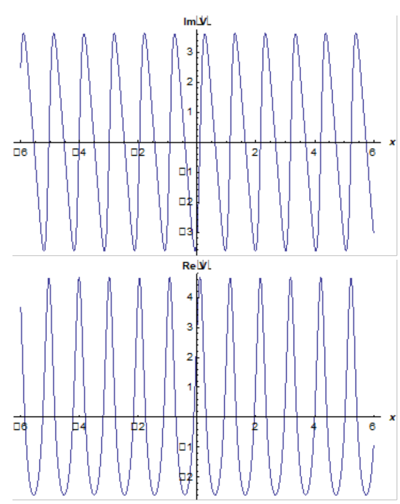

Figure 12: The 2D graphs of Eq. (25) for $a_3 = 0.1$, $d = -0.2$, $b_0 = b_1 = 0.3$, $c = 0.25$, $\delta_1 = \delta_2 = 0.5$, $\alpha = 0.9$, $E = 0.1$, $w_0 = 0.7$, $\omega_0 = 0.8$, $y = 0.03$, $t = 0.5$, $-6 < x < 6$.

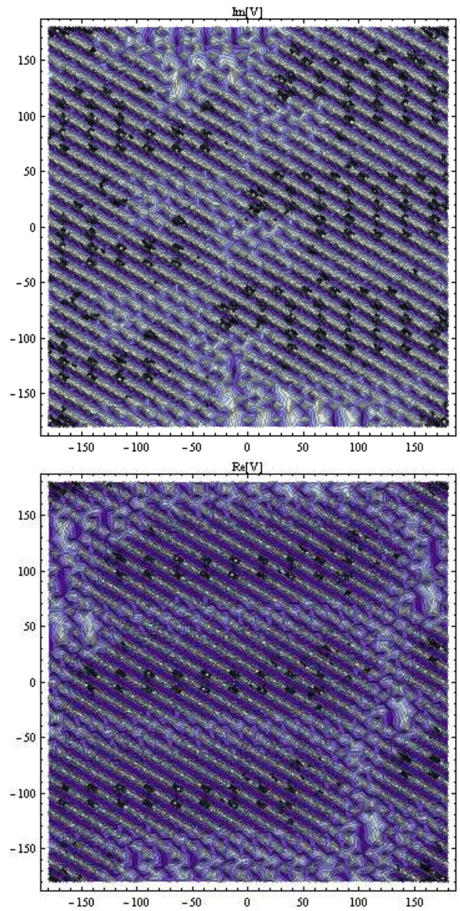

Figure 13: The contour graphs of Eq. (25) for $a_3 = 0.1$, $d = -0.2$, $b_0 = b_1 = 0.3$, $\delta_1 = \delta_2 = 0.5$, $c = 0.25$, $\alpha = 0.9$, $E = 0.1$, $w_0 = 0.7$, $\omega_0 = 0.8$, $y = 0.03$, $-180 < x < 180$, $-180 < t < 180$.

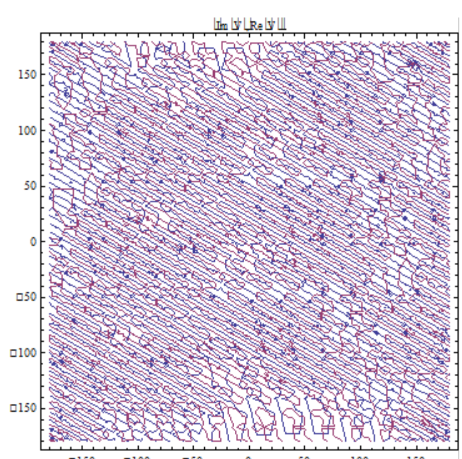

Figure 14: The compilation of contour graphs of both sides of Eq. (25) for $a_3 = 0.1$, $d = -0.2$, $b_0 = b_1 = 0.3$, $\delta_1 = \delta_2 = 0.5$, $c = 0.25$, $\alpha = 0.9$, $E = 0.1$, $w_0 = 0.7$, $\omega_0 = 0.8$, $y = 0.03$, $-180 < x < 180$, $-180 < t < 180$.

4 Conclusions

In this paper, complex dark travelling wave structures that are solutions to Eq. (1) have been extracted by using IBSEFM. Many entirely new solutions such as exponential, rational, dark and the complex exponential have been successfully obtained. It has been observed that all solutions found in this paper have satisfied the nonlinear electrical transmission line model. Choosing suitable values for parameters, better understanding of the physical meanings of the solutions found, and the three- and two-dimensional graphs and contour simulations drawn via computational programs have all been employed.

The perspective view of the solutions Eqs. (19, 21, 23, 25) can be viewed from the 3D, 2D graphs in Figures 1, 5, 7, 11 and Figures 2, 8, 12, respectively. The contour patterns can be also viewed from Figures 3, 6, 9, 13, separately for the imaginary and real part of the solutions. As an alternative and new perspective to the 3D graph, contour surfaces give more detail on the model. Moreover, the contour patterns of combinations of imaginary and real part of the obtained solutions can be seen in Figures 4, 10, 14. When we consider these contour surfaces, it can be observed that the voltage is of high points among intervals in figures as a physical meanings.

Comparing results produced in this paper with the paper published in [7, 8], it can also be seen that Eq. (21) is similar hyperbolic type. Furthermore, it can be observed that the solutions Eqs. (19, 23, 25 are entirely new complex dark solutionsto the nonlinear electrical transmission line model. The calculations show that this method is a reliable and efficient scheme that yields many complex results to the other nonlinear models. To the best of our knowledge, the application of IBSEFM to Eq. (1) has been not submitted to literature in advance.

Acknowledgement: This study was supported by Harran University Scientific Research Projects Department with BAP project code: 16213. In calculations of system, Matlab 2016b version of HPC in Harran University has been used.

References

[1] Senel M., Senel B., Bilir L., Zeytin V., The Relation Between Electricity Demand and the Economic and Demographic State: A Multiple Regression Analysis, The Journal Of Energy And Development, 38(2), 257-274, 2013.

[2] Reda H., Elnady K., Ganghoffer J.F., Lakiss H., Wave propagation in pre-deformed periodic network materials based on large strains homogenization, Composite Structures, 184, 860-871,

2018.
[3] Ma J., Song X., Tang J., Wang C., Wave emitting and propagation induced by autapse in a forward feedback neuronal network, Neurocomputing, 167, 378-389, 2015.
[4] Rostami Z., Pham V.T., Jafari S., Hadaeghi F., Ma J., Taking control of initiated propagating wave in a neuronal network using magnetic radiation, Applied Mathematics and Computation, 338, 141-151, 2018.
[5] Dutykh D., Caputo J.G., Wave dynamics on networks: Method and application to the sine-Gordon equation, Applied Numerical Mathematics, 131, 54-71, 2018,
[6] Aalto A., Malinen J., Wave propagation in networks: a system theoretic approach, IFAC Proceedings Volumes, 44(1), 8854-8859, 2011.
[7] Tala-Tebue E., Zayed E.M.E., New Jacobi elliptic function solutions, solitons and other solutions for the (2+1)-dimensional nonlinear electrical transmission line equation, European Physical Journal Plus, 133(314),1-7, 2018.
[8] Tala-Tebue E., Tsobgni-Fozap D.C., Kenfack-Jiotsa A., Kofane T.C., Envelope periodic solutions for a discrete network with the Jacobi elliptic functions and the alternative (G'/G)-expansion method including the generalized Riccati equation, European Physical Journal Plus, 129(136), 1-10, 2014.
[9] Zheng B., Application of A Generalized Bernoulli SubODE Method For Finding Traveling Solutions of Some Nonlinear Equations, WSEAS Transactions on Mathematics, 7:11, 618-626, 2012
[10] Zheng B., A new Bernoulli sub-ODE method for constructing traveling wave solutions for two nonlinear equations with any order, U. P. B. Sci. Bull., Series A. 73:3, 2011.
[11] Baskonus H.M., Koc D.A., Bulut H., New travelling wave prototypes to the nonlinear Zakharov-Kuznetsov equation with power law nonlinearity, Nonlinear Sci. Lett. A, 7:2, 67-76, 2016.
[12] Bulut H., Demirdag B., Baskonus H.M., Regarding on the Novel Forms of the (3+1) - Dimensional Kadomstev-Petviashvili Equation, ITM Web of Conf, 13(01018) 1 (2017)
[13] Pronin V., Shkatov P., Sandulyak A., Baskonus H.M., Continuous ultrasonic thickness measurement technology, ITM Web of Conf, 13(01026) 1 (2017)
[14] Yokus A., Sulaiman T.A., Gulluoglu M.T., Bulut H., Stability Analysis, Numerical and Exact Solutions of the (1+1)-Dimensional NDMBBM Equation, ITM Web Conf., 22(01064), 2018.
[15] Heydari M.H., Hooshmandasl M.R., Ghaini F.M.M., Cattani C., A computational method for solving stochastic Ito-Volterra integral equations based on stochastic operational matrix for generalized hat basis functions, Journal of Computational Physics, 270, 402-415, 2014.
[16] Sulaiman T. A., Bulut H., Yokus A., Baskonus H. M., On the exact and numerical solutions to the coupled Boussinesq equation arising in ocean engineering, Indian Journal of Physics, 1-10, 2018.
[17] Cattani C., Rushchitskii Ya.Ya., Cubically nonlinear elastic waves: wave equations and methods of analysis, International Applied Mechanics, 39 (10), 1115-1145, 2003.
[18] Seadawy A. R., Modulation instability analysis for the generalized derivative higher order nonlinear Schrödinger equation and its the bright and dark soliton solutions, Journal of Electromagnetic Waves and Applications, 31, 1353-1362, 2017.
[19] Cattani C., Harmonic wavelet solutions of the Schrodinger equation, International Journal of Fluid Mechanics Research, 30(5), 463-472, 2003.
[20] Guedda M., Hammouch Z., On similarity and pseudo-similarity solutions of Falkner–Skan boundary layers, Fluid Dynamics Research, 38(4), 211-223, 2006.
[21] Raza N., Afzal U., Butt A.R., Rezazadeh H., Optical solitons in nematic liquid crystals with Kerr and parabolic law nonlinearities, Optical and Quantum Electronics, 51(4), 107, 2019.
[22] Zhao Z., Han B., Residual symmetry, Böcklund transformation and CRE solvability of a (2+1)-dimensional nonlinear system, Nonlinear Dynamics, 94(1), 461-474, 2018.
[23] Baskonus H.M., New acoustic wave behaviors to the Davey–Stewartson equation with power-law nonlinearity arising in fluid dynamics, Nonlinear Dynamics, 86(1), 177–183, 2016
[24] Cattani C., Abdulkadir Sulaiman T.,.Baskonus H.M, Bulut H., On the soliton solutions to the Nizhnik-Novikov-Veselov and the Drinfel'd-Sokolov systems, Optical and Quantum Electronics, 50(3), 138, 2018,
[25] Awati V.B., Dirichlet series and analytical solutions of MHD viscous flow with suction / blowing, Applied Mathematics and Nonlinear Sciences, 2(2), 341–350, 2017.
[26] Amkadni M., Azzouzi A., Hammouch Z., On the exact solutions of laminar MHD flow over a stretching flat plate, Communications in Nonlinear Science and Numerical Simulation 13 (2), 359-368, 2008.
[27] Cattani C., Abdulkadir Sulaiman T., Baskonus H.M., Bulut H., Solitons in an inhomogeneous Murnaghan's rod, European Physical Journal Plus, 133(228), 1-12, 2018,
[28] Zhao Z., He L., Gao Y., Rogue Wave and Multiple Lump Solutions of the (2+1)-Dimensional Benjamin-Ono Equation in Fluid Mechanics, Complexity, 8249635, 1-18, 2019.
[29] Baskonus H.M., Cattani C., Ciancio A., Periodic, Complex and Kink-type Solitons for the Nonlinear Model in Microtubules, Journal Applied Sciences, 21, 34-45, 2019.
[30] Rushchitsky J.J., Cattani C., Terletskaya E.V., Wavelet analysis of the evolution of a solitary wave in a composite material, International Applied Mechanics, 40(3), 311-318, 2004.
[31] Pandey P.K., A new computational algorithm for the solution of second order initial value problems in ordinary differential equations, Applied Mathematics and Nonlinear Sciences, 3(1), 167–174, 2018.
[32] Eskitascioglu E.I., Aktas M.B., Baskonus H.M., New Complex and Hyperbolic Forms for Ablowitz-Kaup-Newell-Segur Wave Equation with Fourth Order, Applied Mathematics and Nonlinear Sciences, 4(1), 105-112, 2019.